

Mixed Oxides of the Type MO_2 (Fluorite) – M_2O_3 . III.*
Crystal Structures of the Intermediate Phases $\text{Zr}_5\text{Sc}_2\text{O}_{13}$ and $\text{Zr}_3\text{Sc}_4\text{O}_{12}$

BY M. R. THORNER AND D. J. M. BEVAN

School of Chemistry, University of Western Australia, Nedlands, Western Australia

AND J. GRAHAM

Division of Applied Mineralogy, C. S. I. R. O., Wembley, Western Australia

(Received 29 August 1967 and in revised form 23 October 1967)

The structures of the intermediate phases $\text{Zr}_5\text{Sc}_2\text{O}_{13}$ and $\text{Zr}_3\text{Sc}_4\text{O}_{12}$ in the system $\text{ZrO}_2\text{--Sc}_2\text{O}_3$ have been determined from intensity data obtained with a Hägg–Guinier focusing X-ray powder camera and Cu $K\alpha_1$ radiation. The space group in both cases is $R\bar{3}$, and the hexagonal unit-cell dimensions are respectively $a=9.53(2)$, $c=17.44(2)$ Å and $a=9.37(8)$, $c=8.71(0)$ Å. Both these structures are derived from the fluorite-type parent MO_2 by ordered omission of oxygen atoms; the observed rhombohedral distortion is the result of lattice relaxation. It is possible to recognize structural sub-units from which these and other fluorite-related structures can be built up. Such sub-units are likely to play an important role in any adequate description of grossly non-stoichiometric phases.

Introduction

Studies in the binary rare-earth oxide systems MO_x ($M=\text{Ce, Pr, Tb}$; $1.5 < x < 2.0$) have revealed the equilibrium existence of low-temperature, ordered, intermediate stoichiometric phases closely related in structure to the parent fluorite type. Each intermediate phase decomposes peritectoidally (at successively higher temperatures as x decreases) to form, in most cases, another ordered phase with lower x and the disordered, grossly non-stoichiometric α phase, or, in the case of M_7O_{12} , two distinct non-stoichiometric phases, α and σ , whose 'average' structures appear to be fluorite type and rare-earth C type respectively (Bevan, 1955; Brauer & Gradinger, 1954; Bevan & Kordis, 1964; Hyde & Eyring, 1965; Hyde, Bevan & Eyring, 1966). The intermediate phases constitute a homologous series of formula $\text{M}_n\text{O}_{2n-2}$. Their structures have not been determined, although Baenziger, Eick, Schuldt & Eyring (1961) have established the rhombohedral cell of Tb_7O_{12} , and Sawyer, Hyde & Eyring (1965) have reported probable symmetries and pseudo-cells for several $\text{Pr}_n\text{O}_{2n-2}$ phases.

In the non-stoichiometric phases the disorder can no longer be considered as a random distribution of point defects; *i.e.* vacancies or interstitials in the host lattice, and it has been suggested that grossly non-stoichiometric phases at equilibrium are microheterogeneous in character; that they consist of disordered small regions or microdomains of two kinds which differ in both 'structure' and 'composition' yet are coherent in the sense that the degree of misfit across the microdomain boundaries is very small (Wadsley,

1955; Ariya & Popov, 1962; Anderson, 1963; Wadsley, 1963; Anderson, 1964). Implicit in this description is the suggestion that the short-range order which characterizes a microdomain structure is of a kind which also occurs and extends to long range in an ordered stoichiometric phase of the system. To understand the disordered phases, it is therefore important to know the structures of the intermediate ordered phases, and to determine the common structural principle which relates the members of a homologous series.

In most ternary or pseudo-binary systems of the same type (*e.g.* $\text{CeO}_2\text{--Y}_2\text{O}_3$: Bevan, Barker, Martin & Parks, 1965), the non-stoichiometric phases α and σ occur at high temperatures, but no evidence of ordered intermediate phases at lower temperatures has been found. This may be due to the sluggishness of cation rearrangement at temperatures low enough for intermediate phases to be stable, in contrast to the rapidity of electron rearrangement which effects an ordered distribution of +3 and +4 cations in the binary systems. The results of Lefèvre (1963) on the system $\text{ZrO}_2\text{--Sc}_2\text{O}_3$ are therefore of considerable interest since they show the occurrence in this system of three fluorite-related, intermediate phases, β , γ , and δ (Lefèvre's designation). X-ray powder patterns of the γ and δ phases were indexed as hexagonal and rhombohedral respectively. Rather wide compositional widths for these phases were reported although an ideal stoichiometry, $\text{Zr}_3\text{Sc}_4\text{O}_{12}$, was suggested for the δ -phase (Collongues, Queyroux, Perez y Jorba & Gilles, 1965). (Phases of this composition in the binary systems have been designated ι by Hyde, Bevan & Eyring, 1966.) Further work (Bevan & Thorner, to be published), in which samples of the coprecipitated hydroxides were reacted at 1450°C and cooled very slowly over a period of 2–3 weeks, has indicated much narrower composi-

* Part I: Bevan & Kordis (1964).
 Part II: Bevan, Barker, Martin & Parks (1965).

tional widths. This paper reports the determination from X-ray powder data of the structures of γ and δ , from which the ideal formulae Zr₅Sc₂O₁₃ for γ , and Zr₃Sc₄O₁₂ for δ were derived, confirming in the latter case what had been suggested, and proposes a possible structural principle common to fluorite-related intermediate phases of general formula M_nO_{2n-2}.

Structure determination

Diffraction patterns were obtained with a Hagg-Guinier focusing camera and strictly monochromatic Cu K α ₁ radiation. The patterns for each phase were indexed on the basis of a non-primitive hexagonal unit cell with $a_\gamma = 9.53(2)$, $c_\gamma = 17.44(2)$ Å and $a_\delta = 9.37(8)$, $c_\delta = 8.71(0)$ Å. The primitive cell in each case is rhombohedral with $a = 8.00(5)$ Å, $\alpha = 73.0(8)^\circ$ for γ and $a = 6.14(4)$ Å, $\alpha = 99.5(0)^\circ$ for δ : the cell contents are respectively Zr₁₀Sc₄O₂₆ and Zr₃Sc₄O₁₂. Observed (pycnometric) and calculated densities were respectively 5.42 and 5.47 g.cm⁻³ for γ and 4.84 and 4.85 g.cm⁻³ for δ . The integrated diffraction intensities were measured with a planimeter from microdensitometer traces obtained from films exposed for times ranging from 2 to 256 minutes. Corrections were made for the Lorentz and polarization factors, oblique incidence of the diffracted beam on the film, and for sample absorption (Sas & de Wolff, 1966). The combined correction formula is

$$I_{\text{corr}} = \text{const.} \frac{I_{\text{obs}} \sin \theta \sin 2\theta \cos (2\theta - \beta)}{p(1 + \cos 2\alpha \cos^2 2\theta)} \times \frac{\sec \beta - \sec (2\theta - \beta)}{[\exp \{-\mu t \sec (2\theta - \beta)\} - \exp (-\mu t \sec \beta)] [1 - \exp \{-\mu d \sec (2\theta - \beta)\}]}.$$

I_{obs} is the integrated intensity, θ the Bragg angle, β the angle between the incident beam and the normal to the sample surface (30°); α is the Bragg angle for the monochromator ($13^\circ 21'$), μ an appropriate linear absorption coefficient, t and d the thicknesses of the sample and a single emulsion of the film respectively, and p the multiplicity of the reflection. This formula includes a geometric term to take account of the angular-dependent distance between sample and film inherent in the Guinier camera geometry. Following Hellner (1954), the geometric term $\sin 3\theta$ was used instead of the product $\sin 2\theta \cos (2\theta - \beta)$ for the γ -phase data. However, the error introduced was shown to be insignificant.

The powder patterns were obviously fluorite-related, and model structures consistent with the three-dimensional Patterson functions and with the unit-cell contents were obtained in space group $R\bar{3}$. In these models randomized metal atoms, oxygen atoms and 'oxygen vacancies' were distributed over the various equivalent points at the ideal fluorite positions. Refinement was carried out on a P.D.P.6 computer by a block-diagonal least-squares method (Rae, 1966) followed every few cycles by a calculation which reallocated the intensity of each powder line among its constituent reflexions in proportion to the calculated structure factors, in accordance with the requirement of the space group in which mirror and glide planes are absent. Incidental overlap of lines was also allowed for in this calculation.

Table 1. Comparison of final parameters with those of fluorite

All atom positions are for the hexagonal setting of $R\bar{3}$.

| γ -Phase Zr ₁₀ Sc ₄ O ₂₆ | | | | | | | | | | | | |
|--|-----------|-------------|---------------------|--------|-------------|---------------------|--------|-------------|---------------------|--------|-------------|--|
| Atom position | x | $\sigma(x)$ | Fluorite (x) | y | $\sigma(y)$ | Fluorite (y) | z | $\sigma(z)$ | Fluorite (z) | B | $\sigma(B)$ | |
| M(1) | 3(a) | 0.0000 | 0.0000 | 0.0000 | 0.0000 | 0.0000 | 0.0000 | 0.0000 | 0.0000 | 0.70* | — | |
| M(2) | 18(f) | 0.2222 | 0.0003 | 0.1905 | 0.2618 | 0.0003 | 0.2381 | 0.1721 | 0.0002 | 0.1667 | 0.53 | |
| M(3) | 18(f) | 0.2310 | 0.0003 | 0.2381 | 0.0427 | 0.0003 | 0.0476 | 0.3266 | 0.0002 | 0.3333 | 0.88 | |
| M(4) | 3(b) | 0.0000 | 0.0000 | 0.0000 | 0.0000 | 0.0000 | 0.0000 | 0.5000 | 0.0000 | 0.5000 | 0.70* | |
| O(1) | 18(f) | 0.1972 | 0.0016 | 0.1905 | 0.1976 | 0.0015 | 0.2381 | 0.0569 | 0.0009 | 0.0417 | 0.89* | |
| O(2) | 18(f) | 0.2066 | 0.0016 | 0.2381 | 0.0421 | 0.0018 | 0.0476 | 0.2044 | 0.0008 | 0.2083 | 0.89* | |
| O(3) | 18(f) | 0.2161 | 0.0017 | 0.1905 | 0.2572 | 0.0018 | 0.2381 | 0.2929 | 0.0008 | 0.2917 | 0.89* | |
| O(4) | 18(f) | 0.2444 | 0.0018 | 0.2381 | 0.0790 | 0.0016 | 0.0476 | 0.4540 | 0.0008 | 0.4583 | 0.89* | |
| O(5) | 6(c) | 0.0000 | 0.0000 | 0.0000 | 0.0000 | 0.0000 | 0.0000 | 0.3523 | 0.0015 | 0.3750 | 0.89* | |
| δ -Phase Zr ₃ Sc ₄ O ₁₂ | | | | | | | | | | | | |
| Atom position | x | $\sigma(x)$ | Fluorite (x) | y | $\sigma(y)$ | Fluorite (y) | z | $\sigma(z)$ | Fluorite (z) | B | $\sigma(B)$ | |
| M(1) | 3(a) | 0.0000 | 0.0000 | 0.0000 | 0.0000 | 0.0000 | 0.0000 | 0.0000 | 0.0000 | 1.00 | 0.10 | |
| M(2) | 18(f) | 0.2114 | 0.0003 | 0.1905 | 0.2541 | 0.0003 | 0.2381 | 0.3497 | 0.0002 | 0.3333 | 1.26 | |
| O(1) | 18(f) | 0.1900 | 0.0012 | 0.1905 | 0.2117 | 0.0012 | 0.2381 | 0.1142 | 0.0011 | 0.0833 | 1.27 | |
| O(2) | 18(f) | 0.2102 | 0.0012 | 0.2381 | 0.0335 | 0.0012 | 0.0476 | 0.3926 | 0.0011 | 0.4167 | 1.55 | |

* Denotes parameters not refined independently.

Each set of planes was given an individual weight which was determined by the precision of the intensity measurement and the number of independent overlapping

reflexions contributing to the line. Thus the unambiguous $h0l$ reflexions were given a weight of 1, those lines derived from splitting of fluorite lines were given high

Table 2. *Bond lengths and angles*

Primes refer to symmetry related atoms in adjacent asymmetric units.

| γ -Phase $Zr_{10}Sc_4O_{26}$ | | | | | |
|--|---------|----------------|--------|---------------------------------------|--------|
| Polyhedron around metal (1) | | | | | |
| M(1)–O(1) | 2.13 Å | O(1)–O(1') | 2.73 Å | O(1)–M(1)–O(1') | 80.0° |
| Polyhedron around metal (2) | | | | | |
| M(2)–O(1) | 2.08 Å | O(1)–O(2') | 2.53 Å | O(1)–M(2)–O(2') | 71.1° |
| M(2)–O(2) | 2.10 | O(1)–O(2) | 2.99 | O(1)–M(2)–O(4') | 76.2 |
| M(2)–O(3) | 2.11 | O(1)–O(4') | 2.55 | O(2)–M(2)–O(3) | 74.0 |
| M(2)–O(4) | 2.20 | O(2)–O(3) | 2.53 | O(2)–M(2)–O(2') | 77.3 |
| M(2)–O(1') | 3.62 | O(2)–O(2') | 2.73 | O(3)–M(2)–O(4) | 72.6 |
| M(2)–O(2') | 2.27 | O(3)–O(4) | 2.55 | O(3)–M(2)–O(2'') | 74.5 |
| M(2)–O(2'') | 2.28 | O(3)–O(2'') | 2.65 | O(4)–M(2)–O(2') | 74.1 |
| M(2)–O(4') | 2.05 | O(4)–O(2') | 2.69 | O(4)–M(2)–O(4') | 75.6 |
| | | O(4)–O(4') | 2.61 | O(4')–M(2)–O(2'') | 77.0 |
| | | O(4')–O(2'') | 2.70 | | |
| | | O(2)–O(2'') | 3.12 | | |
| | | O(1)–O(2'') | 3.35 | | |
| Polyhedron around metal (3) | | | | | |
| M(3)–O(2) | 2.14 Å | O(2)–O(3) | 2.53 Å | O(2)–M(3)–O(3) | 71.3° |
| M(3)–O(3) | 2.20 | O(2)–O(1) | 2.53 | O(2)–M(3)–O(1) | 72.0 |
| M(3)–O(4) | 2.24 | O(2)–O(3'') | 2.65 | O(2)–M(3)–O(3'') | 73.5 |
| M(3)–O(5) | 2.08 | O(3)–O(5) | 2.51 | O(3)–M(3)–O(5) | 71.7 |
| M(3)–O(3') | 2.06 | O(3)–O(1') | 2.73 | O(3)–M(3)–O(1') | 65.3 |
| M(3)–O(1) | 2.17 | O(4)–O(5) | 2.72 | O(4)–M(3)–O(5) | 77.8 |
| M(3)–O(3'') | 2.29 | O(4)–O(3') | 2.55 | O(4)–M(3)–O(3') | 72.7 |
| M(3)–O(1') | 2.78 | O(4)–O(1') | 2.55 | O(4)–M(3)–O(1') | 59.8 |
| | | O(5)–O(3'') | 2.51 | O(5)–M(3)–O(3'') | 69.8 |
| | | O(3')–O(1) | 2.74 | O(3')–M(3)–O(1) | 80.6 |
| | | O(1)–O(1') | 2.73 | O(1)–M(3)–O(1') | 65.6 |
| | | O(3')–O(3'') | 2.52 | O(3')–M(3)–O(3'') | 70.7 |
| Polyhedron around metal (4) | | | | | |
| M(4)–O(5) | 2.58 Å | O(5)–O(4) | 2.72 Å | O(5)–M(4)–O(4) | 68.7° |
| M(4)–O(4) | 2.21 | O(4)–O(4') | 2.61 | O(4)–M(4)–O(4') | 72.4 |
| Metal–metal distances in asymmetric unit | | | | Average estimated standard deviations | |
| M(1)–M(2) | 3.800 Å | | | M–O distance | 0.02 Å |
| M(2)–M(3) | 3.434 | | | O–O distance | 0.03 |
| M(3)–M(4) | 3.642 | | | M–M distance | 0.004 |
| | | | | O–M–O angle | 0.6° |
| δ -Phase $Zr_3Sc_4O_{12}$ | | | | | |
| Polyhedron around metal (1) | | | | | |
| M(1)–O(1) | 2.13 Å | O(1)–O(1) | 2.74 Å | O(1)–M(1)–O(1) | 79.9° |
| Polyhedron around metal (2) | | | | | |
| M(2)–O(1) | 2.08 Å | O(1)–O(2) | 3.12 Å | O(1)–M(2)–O(1') | 70.4° |
| M(2)–O(1') | 2.55 | O(1)–O(1') | 2.70 | O(1)–M(2)–O(2') | 74.6 |
| M(2)–O(1'') | 2.03 | O(1)–O(2') | 2.61 | O(2)–M(2)–O(1') | 72.1 |
| M(2)–O(2''') | 2.27 | O(1)–O(2'') | 3.00 | O(2)–M(2)–O(2''') | 74.0 |
| M(2)–O(2) | 2.07 | O(2)–O(1') | 2.75 | O(1')–M(2)–O(1'') | 72.6 |
| M(2)–O(2') | 2.22 | O(2)–O(2'') | 2.62 | O(1'')–M(2)–O(2') | 80.6 |
| M(2)–O(2'') | 2.08 | O(2)–O(1'') | 3.18 | O(1'')–M(2)–O(2'') | 74.4 |
| | | O(1')–O(1'') | 2.74 | O(2'')–M(2)–O(2') | 74.7 |
| | | O(1'')–O(2') | 2.75 | O(2'')–M(2)–O(2'') | 73.8 |
| | | O(1'')–O(2''') | 2.61 | | |
| | | O(2'')–O(2') | 2.61 | | |
| | | O(2'')–O(2''') | 2.62 | | |
| Metal–metal distances | | | | Average estimated standard deviations | |
| M(1)–M(2) | 3.761 Å | | | M–O distance | 0.01 Å |
| M(2)–M(2) | 3.421 | | | O–O distance | 0.02 |
| | | | | M–M distance | 0.004 |
| | | | | O–M–O angle | 0.4° |

weights (0.7-0.9), and the remaining superstructure reflexions were given weights of less than 0.5. Provision was made in the intensity reallocation program to increase the relative weighting of these superstructure lines as the refinement proceeded and it became obvious that they were accounted for adequately by the model. Positional parameters of the metals were refined first, followed by those for oxygen. In the next stage temperature factors for the general metal atoms were allowed to vary, and finally all positional parameters were allowed to refine together. Refinement was continued until the calculated shifts were about half the estimated standard deviations. Because of the limited angular range of the reflexions, temperature factors cannot be expected with any accuracy, and oxygen temperature factors were not refined for the γ phase. Atomic scattering factors were taken from the paper by Cromer & Waber (1965).

The choice of space group $R\bar{3}$ was justified by the results; it was felt that because of the limited data available a statistical test for centrosymmetry would be of marginal value.

With maximum use of general positions, only three sensible models could be found for the γ -phase struc-

ture (more if the symmetry were reduced to $R3$). Only one of these refined satisfactorily to give a value of $R = \sum ||F_o| - |F_c|| / \sum |F_o|$ of 0.078 with all reflexions included. In this 36 metal and 72 oxygen atoms were accommodated in positions 18(*f*), 6 metal atoms in positions 3(*a*) and 3(*b*), and 6 oxygen atoms in position 6(*c*) of the hexagonal representation, with the refined parameters shown in Table 1. The use of ionic rather than atomic scattering curves gave a slightly higher R value. Difference-Fourier plots gave no indication at any stage of metal ordering; any attempt to introduce metal ordering into the model for refinement led to an increased R value. The maximum peak height on the final difference-Fourier plot was less than 3% of a metal peak, and interatomic distances and angles (Table 2) were all reasonable. The standard deviations as computed (Table 1) are probably too small because of the optimization of overlapping intensities, but even if they are doubled the result is still good. A total of 27 parameters was refined from the 101 powder intensities measured. Table 3 contains a comparison between observed and calculated intensities.

For the δ -phase only one sensible model in $R\bar{3}$ was obtained. With atomic scattering factors this refined to

Table 3. Observed and calculated values of $\sin^2\theta$ and intensity for the γ phase

| SIN ² θ OBSERVED | SIN ² θ CALCULATED | H | K | L | OBSERVED INTENSITY | CALCULATED INTENSITY | SIN ² θ OBSERVED | SIN ² θ CALCULATED | H | K | L | OBSERVED INTENSITY | CALCULATED INTENSITY | SIN ² θ OBSERVED | SIN ² θ CALCULATED | H | K | L | OBSERVED INTENSITY | CALCULATED INTENSITY | |
|---------------------------------------|---|---|---|----|-----------------------|-------------------------|---------------------------------------|---|---|---|----|-----------------------|-------------------------|---------------------------------------|---|---|---|---|-----------------------|-------------------------|--|
| 0.0105 | 0.0107 | 1 | 0 | 1 | 0.06 | 0.08 | 0.2348 | 0.2350 | 3 | 3 | 0 | 0.35 | 0.57 | | | | | | | | |
| 0.0164 | 0.0165 | 0 | 1 | 2 | 0.01 | 0.02 | 0.2349 | 0.2349 | 4 | 0 | 0 | | | | | | | | | | |
| 0.0177 | 0.0176 | 0 | 0 | 3 | 0.00 | 0.00 | 0.2362 | 0.2364 | 0 | 0 | 0 | 0.93 | 1.19 | | | | | | | | |
| 0.0259 | 0.0261 | 1 | 1 | 0 | 0.16 | 0.19 | | | 3 | 3 | 0 | | | 0.3580 | | | | | | | |
| 0.0365 | 0.0368 | 0 | 2 | 1 | 0.04 | 0.05 | 0.2380 | 0.2380 | 1 | 3 | 0 | 1.45 | 1.46 | | | | | | | | |
| 0.0397 | 0.0399 | 1 | 0 | 4 | 0.39 | 0.39 | 0.2439 | 0.2440 | 0 | 1 | 11 | 0.07 | 0.02 | | | | | | | | |
| 0.0423 | 0.0426 | 2 | 0 | 2 | 0.26 | 0.18 | | | 2 | 4 | 2 | 3.17 | 3.13 | 0.3654 | 0.3655 | | | | | | |
| 0.0435 | 0.0437 | 1 | 1 | 3 | 0.91 | 0.80 | 0.2457 | 0.2458 | 2 | 2 | 4 | | | | | | | | | | |
| 0.0571 | 0.0575 | 0 | 1 | 5 | 0.04 | 0.13 | 0.2518 | 0.2516 | 4 | 2 | 4 | 21.38 | 20.42 | 0.3688 | 0.3686 | | | | | | |
| 0.0626 | 0.0629 | 1 | 2 | 1 | 0.12 | 0.09 | | | 4 | 4 | 1 | | | 0.3751 | 0.3753 | | | | | | |
| 0.0686 | 0.0688 | 1 | 2 | 2 | 43.28 | 42.66 | 0.2534 | 0.2531 | 1 | 4 | 4 | 35.31 | 39.52 | 0.3762 | 0.3764 | | | | | | |
| 0.0702 | 0.0702 | 0 | 0 | 6 | 15.78 | 13.67 | | | 1 | 4 | 6 | | | 0.3931 | 0.3930 | | | | | | |
| 0.0783 | 0.0784 | 3 | 0 | 6 | 0.25 | 0.28 | 0.2563 | 0.2560 | 1 | 2 | 10 | 25.83 | 23.12 | 0.3944 | 0.3947 | | | | | | |
| 0.0836 | 0.0831 | 2 | 0 | 5 | 0.08 | 0.15 | | | 2 | 2 | 10 | | | | | | | | | | |
| 0.0922 | 0.0922 | 2 | 1 | 4 | 14.40 | 15.38 | 0.2609 | 0.2610 | 3 | 2 | 7 | 1.06 | 0.97 | 0.4015 | 0.4014 | | | | | | |
| | 0.0959 | 3 | 0 | 3 | | | 0.2621 | 0.2624 | 2 | 2 | 3 | 0.45 | 0.33 | 0.4059 | 0.4056 | | | | | | |
| 0.0960 | | 1 | 1 | 6 | 1.29 | 1.06 | 0.2643 | 0.2624 | 0 | 4 | 8 | 1.47 | 1.71 | | | | | | | | |
| | 0.0963 | 1 | 1 | 6 | | | 0.2668 | 0.2664 | 5 | 0 | 5 | 0.11 | 0.02 | 0.4097 | 0.4098 | | | | | | |
| 0.1301 | 0.1305 | 2 | 2 | 0 | 0.30 | 0.35 | 0.2717 | 0.2719 | 3 | 1 | 5 | 2.24 | 1.89 | | | | | | | | |
| | 0.1304 | 1 | 0 | 7 | | | | | 4 | 4 | 2 | | | 0.4176 | 0.4180 | | | | | | |
| 0.1094 | 0.1109 | 1 | 2 | 5 | 0.17 | 0.04 | 0.2753 | 0.2750 | 4 | 2 | 4 | 12.32 | 12.05 | | | | | | | | |
| 0.1150 | 0.1151 | 3 | 1 | 1 | 1.47 | 1.50 | 0.2775 | 0.2777 | 1 | 5 | 1 | 1.78 | 1.70 | | | | | | | | |
| 0.1209 | 0.1210 | 2 | 1 | 2 | 0.79 | 0.67 | 0.2810 | 0.2808 | 0 | 0 | 12 | 3.66 | 3.56 | 0.4232 | 0.4234 | | | | | | |
| 0.1217 | 0.1220 | 2 | 2 | 3 | 0.57 | 0.52 | 0.2901 | 0.2902 | 2 | 3 | 8 | 0.40 | 0.17 | 0.4284 | 0.4286 | | | | | | |
| 0.1301 | 0.1304 | 0 | 2 | 7 | 0.29 | 0.38 | 0.2925 | 0.2926 | 4 | 2 | 5 | 1.65 | 1.91 | | | | | | | | |
| 0.1334 | 0.1335 | 0 | 1 | 8 | 1.41 | 1.40 | 0.2971 | 0.2969 | 1 | 2 | 11 | 0.40 | 0.38 | 0.4345 | 0.4343 | | | | | | |
| 0.1413 | 0.1413 | 4 | 0 | 1 | 0.63 | 0.84 | | | 2 | 1 | 11 | | | 0.4386 | 0.4388 | | | | | | |
| 0.1443 | 0.1444 | 3 | 1 | 4 | 0.84 | 0.45 | 0.3011 | 0.3011 | 1 | 5 | 4 | 1.36 | 1.38 | | | | | | | | |
| 0.1469 | 0.1471 | 3 | 4 | 2 | 0.95 | 0.98 | | | 3 | 3 | 6 | | | 0.4432 | 0.4431 | | | | | | |
| 0.1486 | 0.1488 | 3 | 0 | 6 | 1.90 | 1.96 | | | 1 | 1 | 12 | | | 0.4577 | 0.4579 | | | | | | |
| 0.1578 | 0.1580 | 0 | 0 | 9 | 0.05 | 0.01 | 0.3070 | 0.3069 | 1 | 1 | 12 | | | | | | | | | | |
| 0.1596 | 0.1596 | 2 | 0 | 8 | 0.66 | 0.71 | (BLURRED) | | 1 | 1 | 12 | | | | | | | | | | |
| 0.1619 | 0.1619 | 3 | 1 | 5 | 0.73 | 0.76 | 0.3082 | 0.3082 | 1 | 3 | 10 | | | | | | | | | | |
| 0.1675 | 0.1675 | 2 | 3 | 1 | 3.91 | 3.12 | 0.3131 | 0.3132 | 3 | 0 | 5 | 0.08 | 0.02 | 0.4634 | 0.4637 | | | | | | |
| 0.1701 | 0.1705 | 4 | 0 | 4 | 0.05 | 0.02 | 0.3184 | 0.3187 | 5 | 1 | 5 | 1.05 | 0.90 | | | | | | | | |
| 0.1748 | 0.1747 | 2 | 2 | 6 | 0.56 | 0.32 | 0.3238 | 0.3241 | 4 | 3 | 1 | 0.26 | 0.39 | 0.4694 | 0.4689 | | | | | | |
| 0.1813 | 0.1829 | 4 | 1 | 4 | 35.76 | 41.44 | 0.3310 | 0.3310 | 6 | 0 | 3 | 1.29 | 1.69 | 0.4709 | 0.4713 | | | | | | |
| 0.1860 | 0.1866 | 1 | 2 | 8 | 41.58 | 43.79 | 0.3343 | 0.3343 | 4 | 0 | 15 | 0.25 | 0.21 | | | | | | | | |
| 0.1882 | 0.1881 | 0 | 4 | 5 | 0.06 | 0.13 | | | 2 | 2 | 0 | | | 0.4749 | 0.4754 | | | | | | |
| 0.1967 | 0.1967 | 3 | 2 | 4 | 1.93 | 1.95 | 0.3394 | 0.3394 | 2 | 4 | 7 | 1.90 | 1.90 | | | | | | | | |
| | | 4 | 1 | 3 | | | | | 2 | 4 | 7 | | | 0.4805 | 0.4798 | | | | | | |
| | | 4 | 1 | 3 | | | | | 4 | 1 | 4 | | | | | | | | | | |
| 0.2004 | 0.2004 | 4 | 4 | 3 | 0.70 | 1.00 | 0.3410 | 0.3408 | 1 | 4 | 3 | 0.51 | 0.30 | 0.4871 | 0.4882 | | | | | | |
| | | 4 | 4 | 3 | | | | | 1 | 4 | 3 | | | | | | | | | | |
| 0.2036 | 0.2037 | 1 | 0 | 10 | 0.42 | 0.46 | 0.3423 | 0.3425 | 5 | 0 | 8 | 1.30 | 1.16 | | | | | | | | |
| 0.2088 | 0.2082 | 1 | 3 | 7 | 1.60 | 1.67 | 0.3490 | 0.3492 | 3 | 1 | 11 | 0.56 | 0.50 | | | | | | | | |
| 0.2142 | 0.2142 | 2 | 3 | 5 | 1.33 | 1.07 | 0.3529 | 0.3524 | 4 | 3 | 4 | 0.26 | 0.28 | 0.4960 | 0.4950 | | | | | | |
| 0.2195 | 0.2196 | 0 | 5 | 1 | 0.58 | 0.52 | | | 4 | 3 | 4 | | | | | | | | | | |
| 0.2259 | 0.2255 | 5 | 0 | 2 | 0.20 | 0.26 | | | 3 | 3 | 4 | | | | | | | | | | |
| 0.2295 | 0.2298 | 0 | 2 | 10 | 0.34 | 0.41 | | | 3 | 3 | 4 | | | | | | | | | | |

NOT USED IN
STRUCTURE
DETERMINATION

an R value of 0.064. In this model 18 metal and 36 oxygen atoms were accommodated in positions 18(f) and 3 metal atoms in position 3(a) of the hexagonal representation. The parameters and standard deviations are shown in Table 1. Fifteen parameters were refined from the measurement of 50 reflexions (Table 4). Again no evidence for metal ordering was found; the difference-Fourier plot for this structure was even flatter than that for the γ -phase. Bond distances and angles are shown in Table 2. For both phases all the allowed reflexions were observed.

Structural details

Both structures are rhombohedral distortions of the fluorite lattice, one of the four cubic [111] directions becoming the unique inversion triad axis. Fig. 1(a) shows the projection of the fluorite atom positions on the (0001) hexagonal plane which is common to the idealized structures of both γ and δ . All three structures are very similar, but γ and δ show differences of detail due to the different compositions and also to slight differences in the degree of distortion from the ideal. Fig. 1(b) shows for the γ phase the oxygen atoms in the vicinity of a threefold rotation axis chosen to pass through atoms in the A layers of the cubic-close packed sequence. Relative to the MO_2 composition

of fluorite there are six oxygen positions in the hexagonal unit cell which are not occupied. These 'vacancies' are distributed two to each threefold axis so that the special metals lying on these are alternately 6- and 8-coordinated as shown in Fig. 1(b). For the δ phase these special metals are *all* 6-coordinated: *no* oxygen atoms occur in the threefold axis, so that the ideal structure has half the c dimension of the ideal γ phase shown in Fig. 1(b), and its ideal composition is M_7O_{12} . In the fluorite structure *all* oxygen positions in the threefold axis are occupied.

In both the γ - and δ -phase structures the missing oxygen atoms result in 6-coordinated metal atoms at the corners of the rhombohedral unit cell. In the former, the distribution of oxygen 'vacancies' can be described as a diamond lattice in which the 'bonds' parallel to the trigonal axis are shorter (4.36 Å) than the other three (5.69 Å). In the latter structure two such 'vacancy' lattices interpenetrate.

The four different MO_x coordination polyhedra occurring in the γ phase are shown in Fig. 2. The dotted cubes each represent the MO_8 coordination polyhedron of fluorite. Fig. 3 shows the stacking sequence of MO_x polyhedra (represented by cubes) around the threefold axis. With respect to the ideal fluorite positions 6 oxygen atoms coordinating metal (1) have all moved towards the metal and towards the 'oxygen vacancies',

Table 4. *Observed and calculated values of $\sin^2\theta$ and intensity for the δ phase*

| $\sin^2\theta$ OBSERVED | $\sin^2\theta$ CALCULATED | H | K | L | OBSERVED INTENSITY | CALCULATED INTENSITY | $\sin^2\theta$ OBSERVED | $\sin^2\theta$ CALCULATED | H | K | L | OBSERVED INTENSITY | CALCULATED INTENSITY | | |
|----------------------------|------------------------------|-----------|---|----|-----------------------|-------------------------|----------------------------|------------------------------|-----------|-----------|---|-----------------------|-------------------------|------|------|
| 0.0174 | 0.0168 | 1 | 0 | 1 | 0.1 | 0.0 | 0.3105 | 0.3101 | (5 1 -2) | 1 | 5 | 7.5 | 5.5 | | |
| 0.0267 | 0.0270 | 1 | 1 | 0 | 1.1 | 1.0 | | | (3 3 -2) | 3 | 3 | | | | |
| 0.0400 | 0.0405 | 0 | 1 | 2 | 1.1 | 1.6 | | | (3 1 -5) | 3 | 1 | 5.2 | 3.6 | | |
| 0.0435 | 0.0438 | 0 | 2 | 1 | 0.3 | 0.7 | 0.3127 | 0.3124 | (1 3 -5) | 1 | 3 | | | | |
| 0.0672 | 0.0675 | 2 | 0 | 2 | 0.1 | 0.1 | | | (5 2 0) | 5 | 2 | 7.1 | 5.7 | | |
| 0.0672 | 0.0704 | 0 | 0 | 3 | | | | | (2 5 0) | 2 | 5 | | | | |
| 0.0705 | (1 2 -1) | 1 | 2 | -1 | 34.6 | 95.0 | 0.3240 | 0.3238 | 6 | 0 | 0 | 0.4 | 0.1 | | |
| 0.0708 | (2 1 1) | 2 | 1 | 1 | | | 0.3384 | 0.3394 | 0 | 4 | 5 | 0.4 | 0.3 | | |
| 0.0805 | 0.0809 | 3 | 0 | 0 | 0.2 | 0.2 | 0.3400 | 0.3406 | (4 3 -1) | 4 | 3 | 0.4 | 0.1 | | |
| 0.0942 | 0.0942 | (1 2 -2) | 1 | 2 | -2 | 20.0 | 21.7 | | 0.3500 | 0 | 5 | 4 | | | |
| 0.0972 | 0.0974 | (1 1 -3) | 1 | 1 | -3 | 3.6 | 3.4 | 0.3502 | (5 2 0) | 5 | 2 | 0 | | | |
| 0.1077 | 0.1079 | 2 | 2 | 0 | 1.5 | 1.4 | | | (2 5 0) | 2 | 5 | | | | |
| 0.1246 | 0.1247 | (3 1 -1) | 3 | 1 | -1 | 4.2 | 3.2 | 0.3620 | (0 3 6) | 0 | 3 | 6 | | | |
| 0.1341 | 0.1341 | 1 | 0 | 4 | 4.8 | 4.6 | 0.3641 | 0.3640 | (4 3 -2) | 4 | 3 | 5.1 | 6.0 | | |
| 0.1341 | 0.1517 | 4 | 0 | 1 | | | | | (3 4 -2) | 3 | 4 | | | | |
| 0.1514 | (3 0 3) | 3 | 0 | 3 | 6.7 | 5.2 | 0.3665 | 0.3664 | (3 2 -5) | 3 | 2 | 7.7 | 8.2 | | |
| 0.1514 | (5 0 -3) | 5 | 0 | -3 | | | | | (2 3 5) | 2 | 3 | 27.4 | 27.7 | | |
| 0.1611 | 0.1611 | 0 | 2 | 4 | 3.3 | 3.3 | 0.3774 | 0.3770 | (4 2 4) | 4 | 2 | 4 | 27.4 | 27.7 | |
| 0.1749 | 0.1752 | 0 | 4 | 2 | 0.5 | 0.3 | 0.3895 | 0.3895 | (2 2 6) | 2 | 2 | 0.8 | 0.7 | | |
| 0.1785 | (2 2 3) | 2 | 2 | 3 | | | 0.3918 | 0.3922 | 1 | 0 | 7 | 0.4 | 0.4 | | |
| 0.1787 | (2 2 -3) | 2 | 2 | -3 | 1.0 | 1.8 | | | (6 0 3) | 6 | 0 | 3 | | | |
| 0.1787 | (2 3 -1) | 2 | 3 | -1 | | | 0.3942 | 0.3941 | (0 6 3) | 0 | 6 | 3 | 5.6 | 5.0 | |
| 0.1882 | 0.1881 | (2 1 4) | 2 | 1 | 4 | | | | (6 1 -1) | 6 | 1 | -1 | | | |
| 0.1889 | 0.1889 | (4 1 0) | 4 | 1 | 0 | 127.4 | 157.1 | 0.4039 | 0.4039 | (2 1 4) | 2 | 1 | 4 | 4.0 | 3.5 |
| 0.2023 | 0.2022 | (3 2 -2) | 3 | 2 | -2 | 7.5 | 7.5 | | | (1 5 -4) | 1 | 5 | -4 | | |
| 0.2045 | 0.2045 | 0 | 1 | 5 | 2.4 | 2.1 | 0.4191 | 0.4192 | 0 | 2 | 7 | 2.0 | 2.4 | | |
| 0.2318 | (0 5 1) | 0 | 5 | 1 | 1.7 | 1.1 | | | (5 2 3) | 5 | 2 | 3 | | | |
| 0.2421 | (2 0 5) | 2 | 0 | 5 | | | 0.4212 | 0.4211 | (5 2 -3) | 5 | 2 | -3 | 5.7 | 6.5 | |
| 0.2421 | (3 1 4) | 3 | 1 | 4 | | | | | (5 2 -3) | 5 | 2 | -3 | | | |
| 0.2424 | (3 1 4) | 3 | 1 | 4 | | | | | (2 5 -3) | 2 | 5 | -3 | | | |
| 0.2424 | (0 2 4 2 8) | 0 | 2 | 4 | 8.2 | 7.5 | 0.4510 | 0.4517 | 4 | 4 | 0 | 1.4 | 1.6 | | |
| 0.2589 | 0.2585 | (2 1 -5) | 2 | 1 | -5 | | | | (2 1 7) | 2 | 1 | 7 | | | |
| 0.2592 | (4 1 3) | 4 | 1 | 3 | 15.0 | 17.1 | 0.4470 | 0.4462 | (1 2 -7) | 1 | 2 | -7 | | | |
| 0.2596 | (1 4 -3) | 1 | 4 | -3 | | | | | 0.4473 | (4 2 4) | 4 | 2 | 4 | 60.9 | 65.2 |
| 0.2596 | (1 4 -3) | 1 | 4 | -3 | | | | | | (2 4 4) | 2 | 4 | 4 | | |
| 0.2596 | (4 2 1) | 4 | 2 | 1 | | | 0.4484 | 0.4485 | (7 0 1) | 7 | 0 | 1 | | | |
| 0.2596 | (2 4 -1) | 2 | 4 | -1 | | | | | (3 5 1) | 3 | 5 | 1 | | | |
| 0.2596 | (4 2 1) | 4 | 2 | 1 | | | | | (5 3 -1) | 5 | 3 | -1 | | | |
| 0.256 | 0.2562 | 5 | 0 | 2 | 0.7 | 0.0 | 0.4570 | 0.4580 | (4 3 4) | 4 | 3 | 4 | 1.4 | 1.3 | |
| 0.2691 | 0.2690 | 4 | 0 | 4 | 6.4 | 7.0 | | | (4 1 6) | 4 | 1 | 6 | | | |
| 0.2820 | 0.2816 | 0 | 0 | 6 | 24.2 | 24.1 | 0.4708 | 0.4704 | (1 4 6) | 1 | 4 | 6 | 37.5 | 38.0 | |
| 0.2834 | 0.2831 | (2 4 -2) | 2 | 4 | -2 | | | | (4 1 4) | 4 | 1 | 4 | | | |
| 0.2867 | 0.2865 | (3 1 1) | 3 | 1 | 1 | 5.9 | 5.6 | | (0 7 2) | 0 | 7 | 2 | | | |
| 0.2965 | 0.2960 | (3 2 4) | 3 | 2 | 4 | 1.4 | 1.4 | 0.4716 | 0.4719 | (3 5 -2) | 3 | 5 | -2 | | |
| 0.3090 | 0.3085 | (1 1 -6) | 1 | 1 | -6 | 0.7 | 1.6 | 0.4758 | 0.4745 | (3 5 -2) | 3 | 5 | -2 | 0.7 | 1.2 |
| | | | | | | | | | | (1 5 5) | 1 | 5 | 5 | | |
| | | | | | | | | | | (6 2 1) | 6 | 2 | 1 | 0.5 | 0.5 |
| | | | | | | | | | | (2 6 -1) | 2 | 6 | -1 | | |

the $\text{O}(1)\text{-M}(1)\text{-O}(1)$ angle increasing from the ideal value of 70.52° to 80.0° . These adjustments are expected to compensate for the two 'oxygen vacancies'. Similarly the neighbouring oxygen atoms have all moved towards the 'oxygen vacancy' in the coordination shell of metal (2) which becomes 7-coordinated. In addition a second-nearest neighbour has moved up almost to within bonding distance. Metals (3) and (4) are 8-coordinated; in the former, one oxygen atom has moved away about 0.6 \AA from the metal whereas in the latter all the M-O distances have increased. These results fit the general observation that the lower the coordination number the shorter are the M-O distances. The distance $\text{M}(1)\text{-M}(2)$ (across an 'oxygen vacancy') is increased by mutual repulsion to 3.80 \AA , whereas the $\text{M}(3)\text{-M}(4)$ distance (3.64 \AA) is what would be expected in a fluorite array.

The rhombohedral distortion thus appears to be due entirely to the 'oxygen vacancies', and there is no evidence to suggest metal ordering as a cause. The changes are all rational, and the movements of the oxygen and the metal atoms can be explained on electrostatic and steric grounds. Because of the similar ionic radii of scandium and zirconium, ordering would only be expected on the basis of charge differences, and the result suggests that the structure may not be strongly ionic in character, in agreement with the better results obtained using atomic scatterers.

In the δ phase only $\text{M}(1)\text{O}_6$ and $\text{M}(2)\text{O}_7$ (see Fig. 4) coordination polyhedra occur. Within the limits of the estimated standard deviations, the $\text{M}(1)\text{O}_6$ polyhedra in both γ and δ are identical. The $\text{M}(2)\text{O}_7$ polyhedra in the two phases are, however, significantly different, although in both cases there is the now familiar movement of neighbouring oxygen atoms towards the 'oxygen vacancy', and in general the metal-metal and metal-oxygen interrelationships are similar to those of the γ phase. Furthermore, there is a difference in the stacking sequence of these polyhedra around the

threefold axis (Fig. 3); for the δ phase this can be represented as 1, 2, 2, 1 (*cf.* 1, 2, 3, 4, 3, 2, 1 for the γ phase).

Discussion

The γ -phase structure has not been reported previously. Indeed, apart from this study and the work of Lefèvre

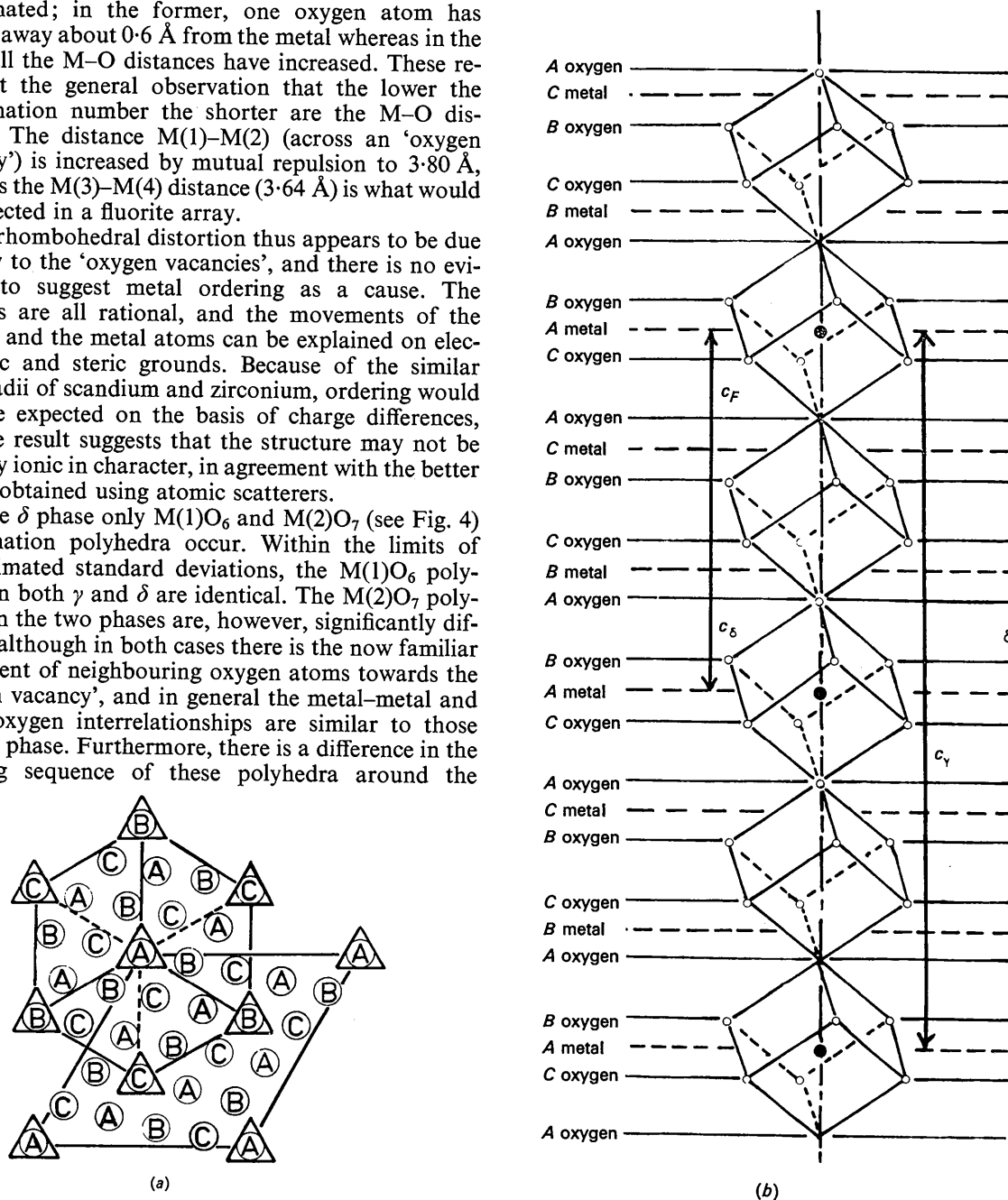


Fig. 1. (a) Projection of the fluorite atom positions on the (001) hexagonal plane. The unit cell shown is common to the ideal structures of both γ and δ . (b) The stacking sequence of metal and oxygen layers, and the atoms in the vicinity of a threefold rotation axis chosen to pass through A atom sites for the γ phase. The c dimensions of the idealized γ structure, fluorite and δ are also shown. In fluorite all oxygen sites in this axis are occupied; in δ all are vacant.

(1963), the only other compound of this formula (M_7O_{13}) and similar unit-cell dimensions is the oxynitride $Zr_7O_{11}N_2$ described briefly by Gilles (1964). It seems possible that Bartram's (1966) 'rhombohedral 2' phase in the system $U + Y + O$ is also analogous. The composition range given is $U_2Y_5O_{13.5}$ to $U_{1.75}Y_{5.25}O_{13.1}$ although the unit cell quoted is similar to that of the 'rhombohedral 1' phase (UY_6O_{12}).

The δ phase in the ZrO_2 - Sc_2O_3 system is apparently isomorphous with the phases $Zr_7O_8N_4$ (Gilles, 1964), $Zr_3Tm_4O_{12}$ and $Zr_3Yb_4O_{12}$ (Bevan & Thornber, to be published), although evidence of cation ordering in $Zr_3Yb_4O_{12}$ has been obtained and might be expected as the sizes of the two cations become less similar. Essentially the same structure was reported for the phases $XO_3 \cdot 3M_2O_3$ [$X = Mo, W, U$; $M = \text{rare-earth}$: Bartram (1966)], and has long been accepted for the M_7O_{12} ($M = Ce, Pr, Tb$) compounds of the binary rare-earth oxide systems (Baenziger *et al.*, 1961). In the former, the cations are ordered, the X atoms being 6-coordinated and the M atoms 7-coordinated; in the latter, at least partial cation ordering into the 6-coordinated site is likely because of the considerable difference between the sizes of the +4 and +3 cations: complete ordering would involve a reduction in symmetry, at least to R3.

A structural feature of all these isomorphous, M_7O_{12} phases is the existence of infinite *strings* of 6-coordinated cations along the threefold axes, which are surrounded by contiguous sheaths of 7-coordinated cations. The 'anion vacancies' in the ideal fluorite structure lie on those body-diagonals of $M(1)O_6V_2$ cubes ($V = \text{vacancy}$) which are threefold axes.

These same infinite strings of 6-coordinated cations are present in the C-type rare-earth oxide (M_2O_3) structure, but lie along all four [111] cubic directions and interweave so that two 'oxygen vacancies', one from each of two strings, lie across the face-diagonal of an $M(2)O_6V_2$ fluorite cube (Fig. 5). In this structure therefore there are two kinds of 6-coordinated cations—those in the strings, $M(1)$ ($\frac{1}{4}$ of the total), and the $M(2)$ cations ($\frac{3}{4}$ of the total), whose 6-coordination results simply from the manner in which the strings interweave.

In the light of these considerations it was proposed (Hyde & Eyring, 1965; Hyde, Bevan & Eyring, 1965) that the string is the structural entity generating the homologous series of fluorite-related phases M_nO_{2n-2} , and model structures for Pr_9O_{16} and $Pr_{12}O_{22}$, based on this principle and consistent with the observed powder diffraction data from well-ordered samples, have been put forward (Sawyer *et al.*, 1965).

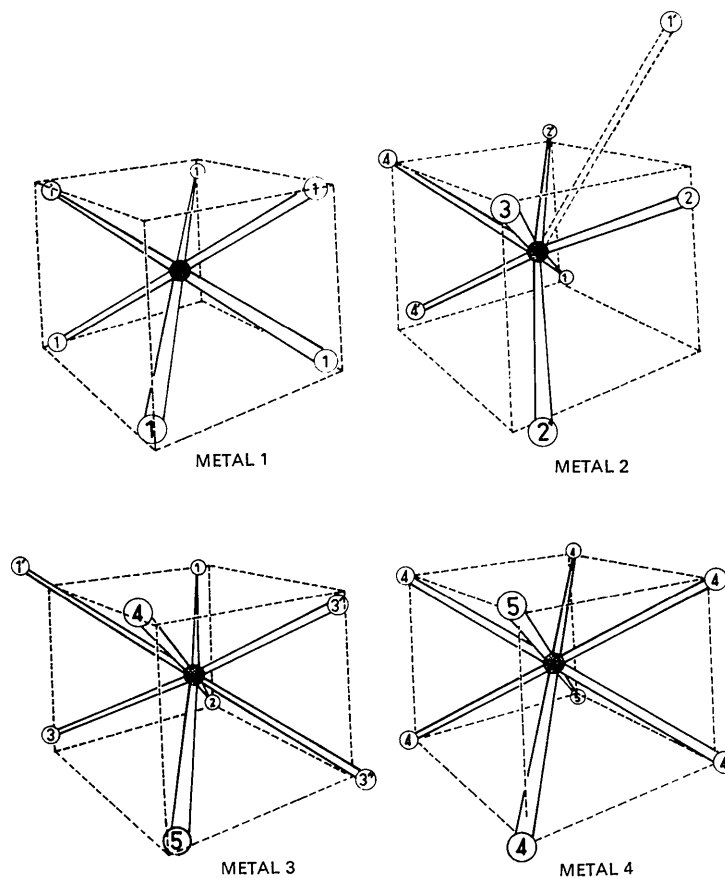


Fig. 2. Metal atom coordination polyhedra in the γ phase. Dotted lines represent the cubic coordination of the fluorite lattice. The metal (1) polyhedron is the same in both γ and δ .

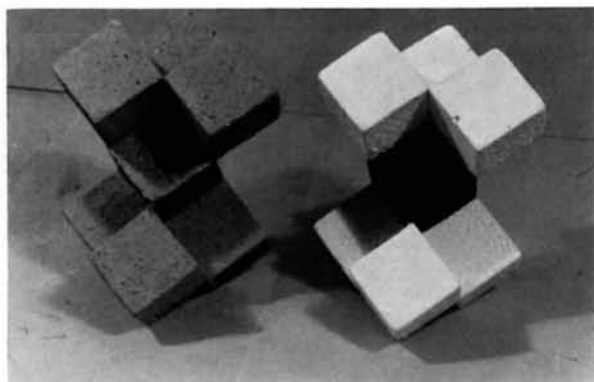


Fig. 6. *7F* (left) and *I* (right) units.

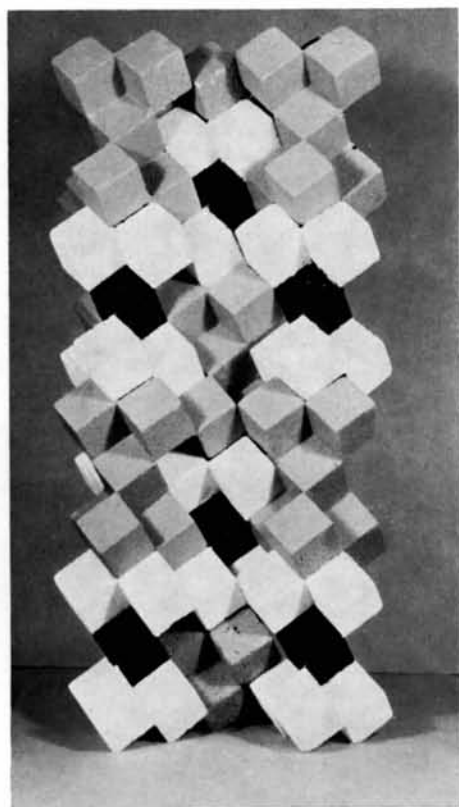


Fig. 7. γ Phase – interpenetrating networks of *I* and *7F* units.

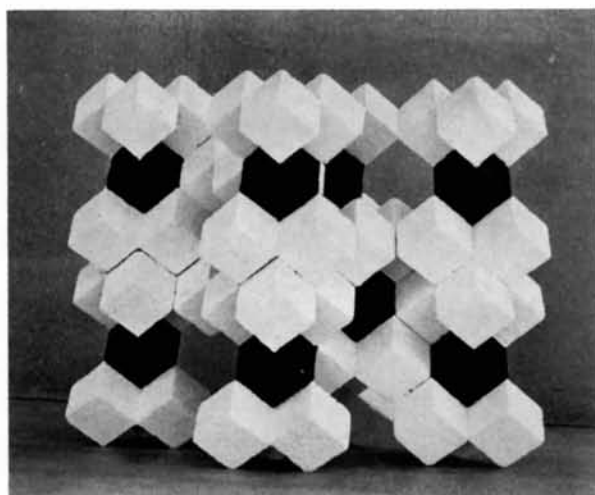


Fig. 8. δ Phase – built up entirely of *I* units.

It now appears that this proposal is not entirely correct; the structure of $\text{Zr}_5\text{Sc}_2\text{O}_{13}$ ($n=14$ of the series) as reported here does not contain these strings. The basic units are rather a 6-coordinated cation associated with six 7-coordinated anions (M_7O_{36} ; designated I), and a similar grouping of 8-coordinated cations which is simply seven edge-sharing MO_8 units of fluorite (M_7O_{38} ; designated $7F$). These are depicted in Fig. 6. The γ -phase structure is built up by edge-sharing of equal numbers of I and $7F$ units all oriented parallel to the threefold axes, and consists of interpenetrating networks of two kinds which fill space as shown in Fig. 7. In the δ -phase structure (Fig. 8) there are only fully edge-shared I units all oriented parallel to the threefold axes. For both structures the relationship to fluorite is evident. The existence of strings is simply a consequence of this latter and other types of edge-sharing of I units inherent in the idealized structures postulated for Pr_9O_{16} and $\text{Pr}_{12}\text{O}_{22}$ (Sawyer *et al.*, 1965; Hyde & Eyring, 1965). The basic structural principle in all these $\text{M}_n\text{O}_{2n-2}$ phases, however, appears to be the ordered arrangement of edge-sharing I and xF units (where x is an integer which may vary from one structure to another): they consist of coherent, ordered regions or microdomains of M_7O_{12} and MO_2 (fluorite).

This microdomain description can be extended to include the stable, high-temperature non-stoichiometric phases σ (C type) and α (fluorite type). These have been observed although not yet clearly delineated in the zirconia-rare-earth oxide systems, but are well-defined in other closely related ternary systems. The structure of the β phase in the system $\text{ZrO}_2\text{-Sc}_2\text{O}_3$ also needs to be determined in the above context and this is presently being investigated.

The authors express their gratitude to Drs E. N. Maslen, B. G. Hyde and A. D. Wadsley for much helpful advice and comment, and to the Australian Atomic Energy Commission for financial support under Contract 65/K/4.

References

- ANDERSON, J. S. (1963). *Advanc. Chem.* **39**, 1.
 ANDERSON, J. S. (1964). *Proc. Chem. Soc.* p. 166.
 ARIYA, S. M. & POPOV, YU. G. (1962). *J. Gen. Chem. Moscow*, **32**, 2077.
 BAENZIGER, N. C., EICK, H. A., SCHULDT, H. S. & EYRING, L. (1961). *J. Amer. Chem. Soc.* **83**, 2219.
 BARTRAM, S. F. (1966). *Inorg. Chem.* **5**, 749.
 BEVAN, D. J. M. (1955). *J. Inorg. Nucl. Chem.* **1**, 49.
 BEVAN, D. J. M., BARKER, W. W., MARTIN, R. L. & PARKS, T. C. (1965). *Rare Earth Research*, **3**, 441. New York: Gordon and Breach.
 BEVAN, D. J. M. & KORDIS, J. (1964). *J. Inorg. Nucl. Chem.* **69**, 480.
 BRAUER, G. & GRADINGER, H. (1954). *Z. anorg. Chem.* **277**, 89.
 COLLONGUES, R., QUEYROUX, F., PEREZ Y JORBA, M. & GILLES, J.-C. (1965). *Bull. Soc. chim. Fr.* p. 1141.
 CROMER, D. T. & WABER, J. T. (1965). *Acta Cryst.* **18**, 104.
 GILLES, J.-C. (1964). *Corrosion et Anticorrosion*, **12**, 15.

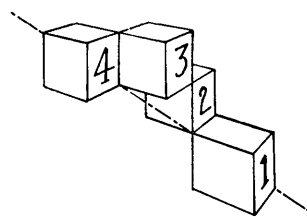


Fig. 3. The stacking sequence of polyhedra shown in Fig. 2. The number on the cube refers to the number of the metal atom contained within that cube.

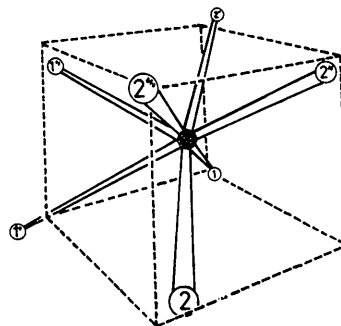


Fig. 4. Metal (2) coordination polyhedron in the δ phase.

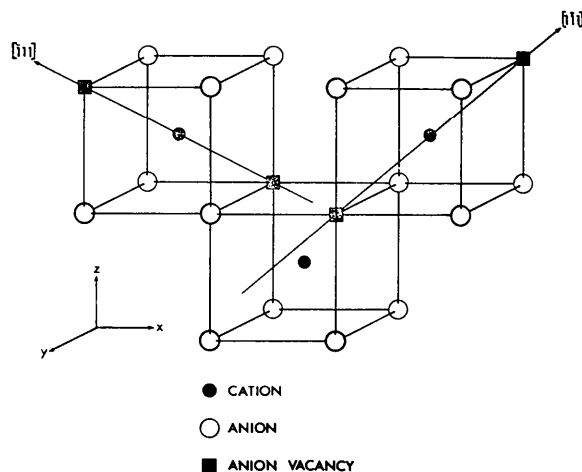


Fig. 5. Interweaving $\text{M}(1)\text{O}_6$ strings in the cubic C -type M_2O_3 structure.

- HELLNER, E. (1954). *Z. Kristallogr.* **106**, 125.
 HYDE, B. G., BEVAN, D. J. M. & EYRING, L. (1966). *Phil. Trans. A* **259**, 583.
 HYDE, B. G., BEVAN, D. J. M. & EYRING, L. (1965). *Intern. Conf. Electron Diffraction and Crystal Defects*, Melbourne, II, C-4.
 HYDE, B. G. & EYRING, L. (1965). *Rare Earth Research*, **3**, 623, New York: Gordon and Breach.
 LEFÈVRE, J. (1963). *Ann. Chim.* **8**, 135.
 RAE, A. I. M. (1966). *World List of Cryst. Comp. Programs*, 2nd ed., p. 32.
 SAS, W. H. & DE WOLFF, P. M. (1966). *Acta Cryst.* **21**, 826.
 SAWYER, J. O., HYDE, B. G. & EYRING, L. (1965). *Bull. Soc. chim. Fr.* p. 1190.
 WADSLEY, A. D. (1955). *Rev. Pure Appl. Chem.* **5**, 165.
 WADSLEY, A. D. (1963). *Advanc. Chem.* **39**, 23.